scientific reports

Check for updates

OPEN

Discovering the dynamics of peach fruit mycobiome throughout fruit development season by high-throughput sequencing

Sibel Öncel[1] & Hilal Özkılınç[1,2]✉

The mycobiome is comprised of a rich array of fungal species that compete for resources, and species diversity and prevalence exhibit a dynamic structure under the influence of many factors. While the host fruit develops, the prevalence and the arrangement of fungal species in this mycobiome also change, forming a dynamic microenvironment. In this study, fungal diversity on peach fruit surfaces at different developmental stages have been determined to better understand the changes in fungal diversity and disease occurrence by using metabarcoding of the full ITS region and processing the obtained high-throughput sequencing data with various bioinformatic analyses. It has been found that fungal diversity in early developmental stages is higher, and the diversity declines as the fruit matures, likely due to more prevalent fungal species establishing themselves on the surface as the fruit develops. Additionally, this research reveals that the prevalence of pathogens does not necessarily mean that disease will develop, as pathogenic species were found to be at higher prevalence percentages when compared to non-pathogenic species in healthy fruit samples. This study also identified the *Monilinia polystroma* species at a molecular level for the first time in Türkiye; however, no symptomatic signals were recorded on the host. The study provides valuable data for mycobiome studies, while also highlighting its importance in optimizing sustainable disease management strategies.

Keywords Fruit mycobiome, Fungal diversity, *Prunus persica*, Metabarcoding, Bioinformatics

Mycobiome is defined as the collection of fungal species present in a specific environment of the host at a certain time[1]. The fungal species forming the mycobiome vary in their taxonomy, belonging to different families and phyla, as well as differing lifestyles such as pathogenic, mutualistic, and saprophytic[2,3]. These fungal species can coexist in the same microenvironment, interact with each other, and affect each other's nutrient uptake, growth, pathogenicity, and resistance to external factors.[4,5]. These effects can also cause unknown or potentially pathogenic species to arise in the mycobiome that take advantage of the absence of other species[6,7]. Although the mycobiome content is constantly fluctuating, the changes that occur within this microenvironment become even more clear with the host's development[8,9].

To understand disease occurrence and develop effective and alternative management strategies for fungal plant diseases, it is essential to understand the content of species and the interactions among these species within the mycobiome[7,10]. Several studies have been reported on uncovering the fungal content of host surfaces, especially of agriculturally important fruits such as apples[11], grapes[12], pineapple[9] and blueberry[13]. Although these studies have shown that several different fungal pathogens are present together on the fruit surface at a time, fluctuations within the mycobiomes were left uncovered, and researchers highlight the importance of gaining more information on dynamics of fungal prevalence. Following this point, some studies have been performed to reveal the mycobiome of fruits throughout the development of the host which were performed on dates[14], and avocados[15]. Both studies report several dominant pathogenic fungal species within the mycobiome at the developed stages of the fruits and indicate the importance of studying fungal diversity of the mycobiome.

When the target of the research is to detect the diversity within an environment, it is important to select the method of isolation and sequencing, and although research has been performed with culture-dependent methodologies before, it is essential to detect the maximum number of species in an environment through

[1]MSc Program in Molecular Biology and Genetics, School of Graduate Studies, Çanakkale Onsekiz Mart University, Çanakkale, Türkiye. [2]Department of Molecular Biology and Genetics, Faculty of Science, Çanakkale Onsekiz Mart University, Çanakkale, Türkiye. ✉email: hilalozkilinc@comu.edu.tr

culture-independent methods that implement high-throughput sequencing techniques[6]. By implementing these methods, mycobiome structure detection can be performed on different economically important agricultural produce.

In Türkiye, peach (*Prunus persica*) has an important economic role in agricultural practices with approximately 1 million tones being produced each year[16]. Although management strategies, mainly fungicides of different active groups, are applied, the cultivars still lose a consequential part of the produce to fungal diseases[17]. Especially the brown rot disease is known as one of the major fungal problems in yield quality and quantity on peach production[18]. This concept makes research discovering the fungal interactions on the host fruit and the fluctuations that occur throughout the season indispensable for agricultural practices. However, studies focusing on the peach fruit mycobiome are lacking in literature, with only one research presenting the microbial diversity of mummified peach fruits[19] and some others focusing on the peach tree wood[20,21] and soil microbiomes[22]. These studies focus on microbial diversity at only one point in time, and report of the fungal species found but the dynamicity and the species fluctuations remain unknown.

In this study, the peach fruit mycobiome was profiled through different host development stages using culture-independent metabarcoding with high-throughput sequencing as well as with an optimized bioinformatics pathway to (I) explore the content of the peach fruit mycobiome, (II) determine the pathogenic fungal species present in the microenvironment at different times to reveal potential disease factors, and (III) discover the fungal prevalence fluctuations across different times. This research fills the knowledge gap regarding mycobiome fluctuations on the surface of peach fruit and provides important insights into the relationship between fungal species abundance and disease development. It also identifies pathogenic species even in the absence of symptoms, shedding light on their potential impact on plant health.

Results

Sampling and mycobiome composition

Peach fruit surface samples were collected each month during different development stages of the host fruit and the samples were sequenced using paired end NovaSeqX 150 bp after total DNA isolation. A mean value of 21,150,34 reads were obtained from the sequencing and a minimum of 93.43% of sequences passed the filtering steps and denoising raw data workflow. The forward and reverse reads were joined by DADA2[23] "merge" function. Success of sequencing on detecting diversity was confirmed by the alpha rarefaction plot (Fig. 1). Taxonomic assignment of the sequences was performed with a newly trained, dynamic Naive-Bayes feature classifier which was successful in detecting all the ASVs present in the data pulled from the UNITE 9.0 database in the classifier evaluation steps, which was then used on the research data. Taxonomic assignments of the samples represented in Fig. 2 showed that *Ascomycetes* were in majority compared to *Basidiomycetes* with an 8:23 ratio. The most prevalent fungal species across all samples and their mean abundance were as follows: the pathogenic species *Botrytis cinerea* (40.3875%), *Monilinia fructicola* (38.7927%), *Sclerotinia sclerotiorum* (7.38282%), *Monilinia polystroma* (2.35553%) and the non-pathogenic *Sporobolomyces roseus* (6.57153%). *Botrytis cinerea* had the highest abundance of 63,106% in the sample taken from the infected fruit in June (the sample J3). At the same time, this sample had the lowest *Monilinia fructicola* abundance with 28.863%. Similarly, when *Monilinia fructicola* abundance was the highest at 51.880%, which was in the A6 sample, *Botrytis cinerea* abundance was at its lowest at 21.805%. Additionally, *Sclerotinia tetraspora*, a monotrophic species in the *Sclerotinia* genus and in close relationship with *S. borealis*[24] was also only found in the infected fruit sample with a percentage of 1.424%.

Sporobolomyces roseus, the only *Basidiomycete* in the most prevalent species criteria, however, was found in a higher percentage in the August samples with an average of 10.6229% than in the June samples where the species abundance percentage average was 1.72786%.

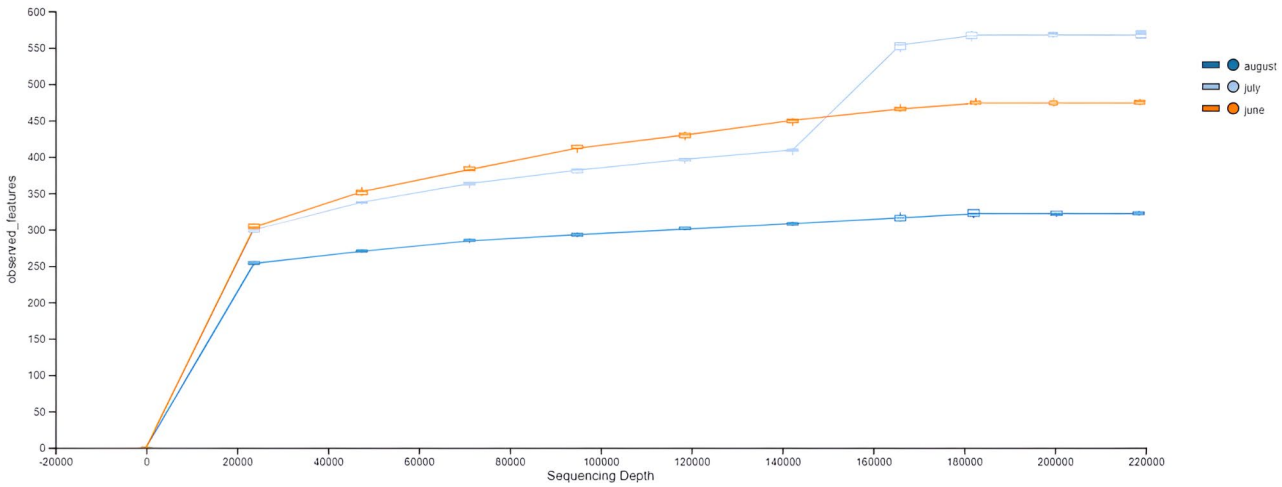

Fig. 1. Alpha rarefaction plot of the sample groups, showing ASV counts per sequence depth.

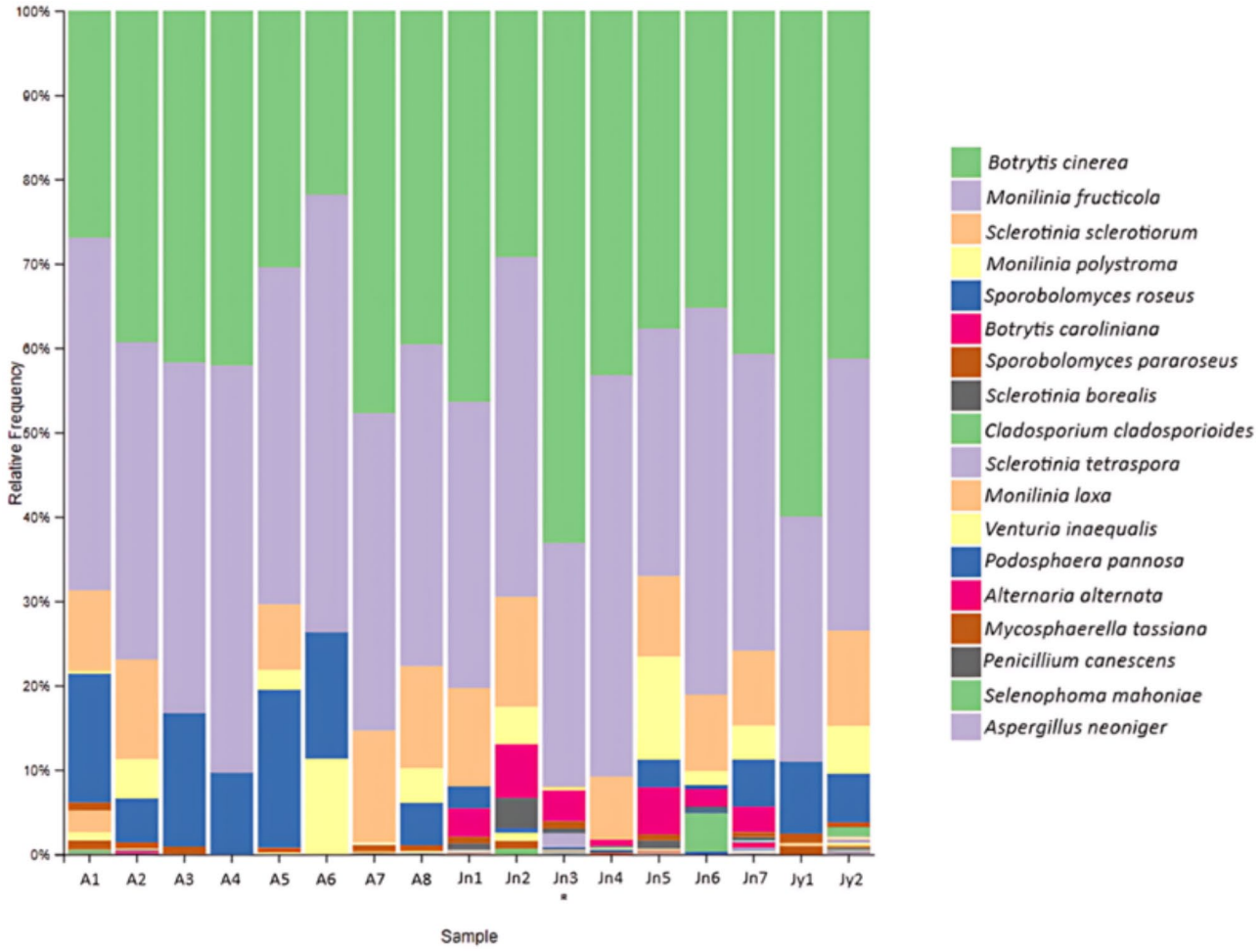

Fig. 2. Taxonomic annotation bar plot and abundance percentages of dominant fungal species in June, July, and August samples (Asterisks (*) indicates the sample including the diseased fruits).

Along with these most prominent species, the mycobiome of all samples also included uncommon species that occurred with percentages lower than 0.5%. The rare species to prevalent species ratio was 15:16, and most of these rare species were present on samples among the June group with an average of 0.01114%.

Alpha and beta diversities of mycobiome profiles

To determine the efficiency of sequences in representing biodiversity within the samples, the alpha rarefaction curve was calculated. This rarefaction curve was also used to select the "maximum depth" of sequences in diversity analyses. The rarefaction curve showed that the observed ASV value of 599 was reached and a plateau was formed at 180,000 reads. As the sequences contained a minimum of 2,115,034 reads, this result showed that the sequences were sufficient in representing the fungal diversity within the samples (Fig. 1). The 180,000 reads were then used in the calculation of diversity indexes.

For alpha diversity, the sample groups' richness and diversity were first calculated using the Shannon index (Fig. 3). The results showed that the fungal mycobiome of the June samples was significantly ($P=0.006$) richer than the August samples, with the mean Shannon entropies with 6.1 and 6.4, respectively (Fig. 3). The Shannon index also showed that the June samples were closer in richness to the July samples than the August samples. The Berger-Parker dominance index was calculated to determine the relative richness of the prevalent species and the extent of a species dominance over the mycobiome (Fig. 3). The diversity richness was lower in August as observed in the Supplementary Material 1, but the dominance index of this group was significantly ($P=0.009$) higher than June's and July's with the mean Berger-Parker dominance index values of 0.027 for August, 0.024 for July, and 0.021 for June (Fig. 3). This result shows that the species dominance over others gradually increased until the host reached the ripe stage.

For beta diversity analyses and beta group significances, the Dice index was used to calculate the similarities between the sample groups according to their species composition (Fig. 4). The index calculation showed that both June and July samples were significantly ($P=0.016$) dissimilar to the August samples, while the June sample group was more similar to the July samples than the August samples. The Jaccard index calculation that compares sample groups based on their shared and unique features showed that June and July samples had significantly

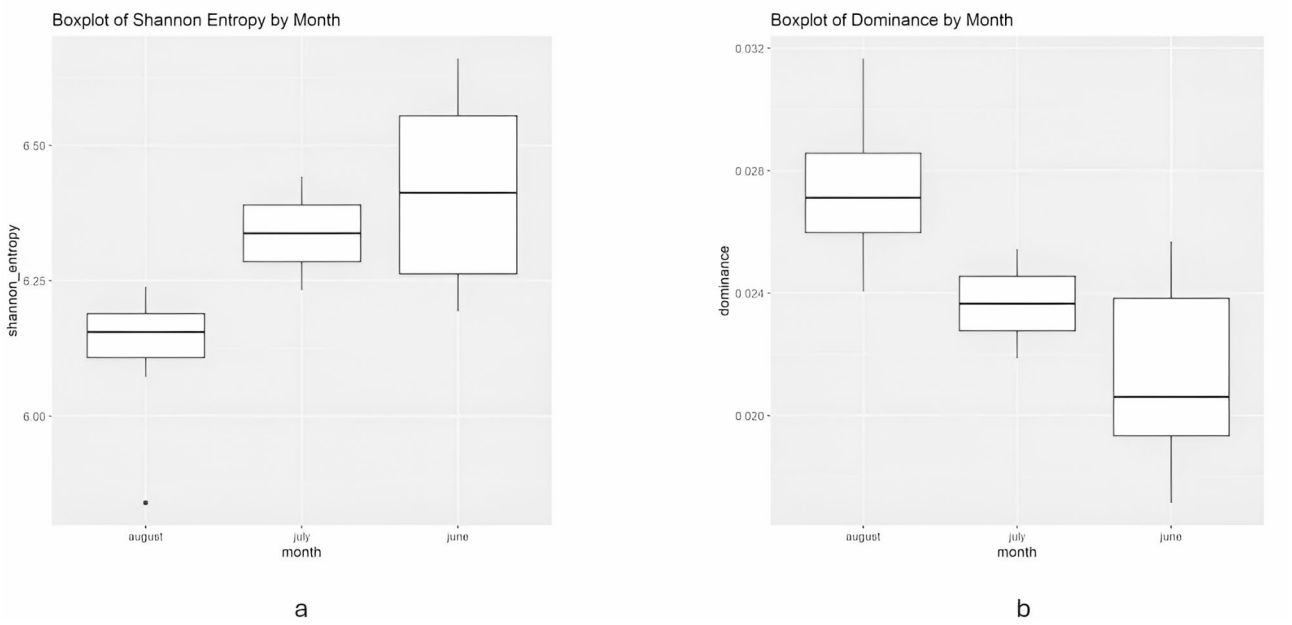

Fig. 3. Box-plots representing α-diversity indexes of Shannon ($P = 0{,}006$) (**a**) and Berger-Parker dominance ($P = 0{,}009$) (**b**) analysis tests.

($P = 0.018$) higher unique features than the August samples (Fig. 4). However, the unique features of the June group were also dissimilar to the July group.

The PCoA proximity patterns based on beta diversity dissimilarities among samples showed close clustering among August samples while June samples were scattered (Fig. 5). The infected sample Jn3 also showed distant diversity index than the other June samples. The distance of the samples was based on the diversity indexes, therefore the July samples proximity patterns showed to be distant from each other.

Phylogenies of fungal species

The phylogenetic tree build resulted in a complicated tree with a quite large cluster count, which was made interpretable by clustering the sequences that belong to the same species together. The "taxa" term given in each cluster refers to the number of sequence variants the species on the branch has which derived from the sequence data and the ASV counts. The cluster sizes were not proportional to the abundance rate of the species, which may be due to prevalent species taxa groups being formed of uniform sequences. The tree showed that the more prevalent species, which are mostly pathogenic and are in the *Leotiomycetes* class, are evolutionarily closer to each other than the rare and/or non-pathogenic species. The tree also included species that were present in the mycobiome at a rate lower than 0.5%, which showed that the populations of rare species groups in the microenvironment were diverse. While some of these species were closely related and grouped into one clade, most were separated into far different branches. Because the phylogram is so large to present here, it is provided as Supplementary Material (S2).

Co-occurrence network analysis

To obtain the total interactions among the species, samples throughout the season were presented in the network analysis (Fig. 6). Co-occurrence network analysis of the ASVs resulted in a network with 48 nodes and 592 edges, with a network density of 0.430. The nodes clustered into 8 modules, with module 1 containing the most interconnected nodes. Additionally, module 1 included the most abundant species' nodes, with both *Botrytis cinerea* and *Monilinia fructicola* being in module 1. Modules 1, 2, 3 and 5 were clustered closely, while the other modules scattered around the network, and mainly interacted with few species in the main cluster, while also having fewer interactions within the module as well. It was also observed that modules 1, 2 and 3 mainly contained mycelial pathogenic fungi while the scattered modules 4, 6, 7 and 8 included mainly yeasts, mutualistic mycelial fungi and/or basidiomycetes.

Discussion

In this study, the fungal diversity appearing on peach fruits during different fruit developmental stages during a season has been characterized and compared by using the metabarcoding and bioinformatics tools. The fruit surface mycobiome is a diverse and dynamic structure that is under many biotic and abiotic stresses[15,25]. Many fungal species with different life cycles are present in this structure, and it is important to incorporate culture-independent studies, along with developing high throughput sequencing techniques to discover the properties of the mycobiome[26–28]. The fungal mycobiome of the peach fruit showed significant differences in the abundance of species across sampling times considering the fruit ripening stages and decrease in fungal diversity was

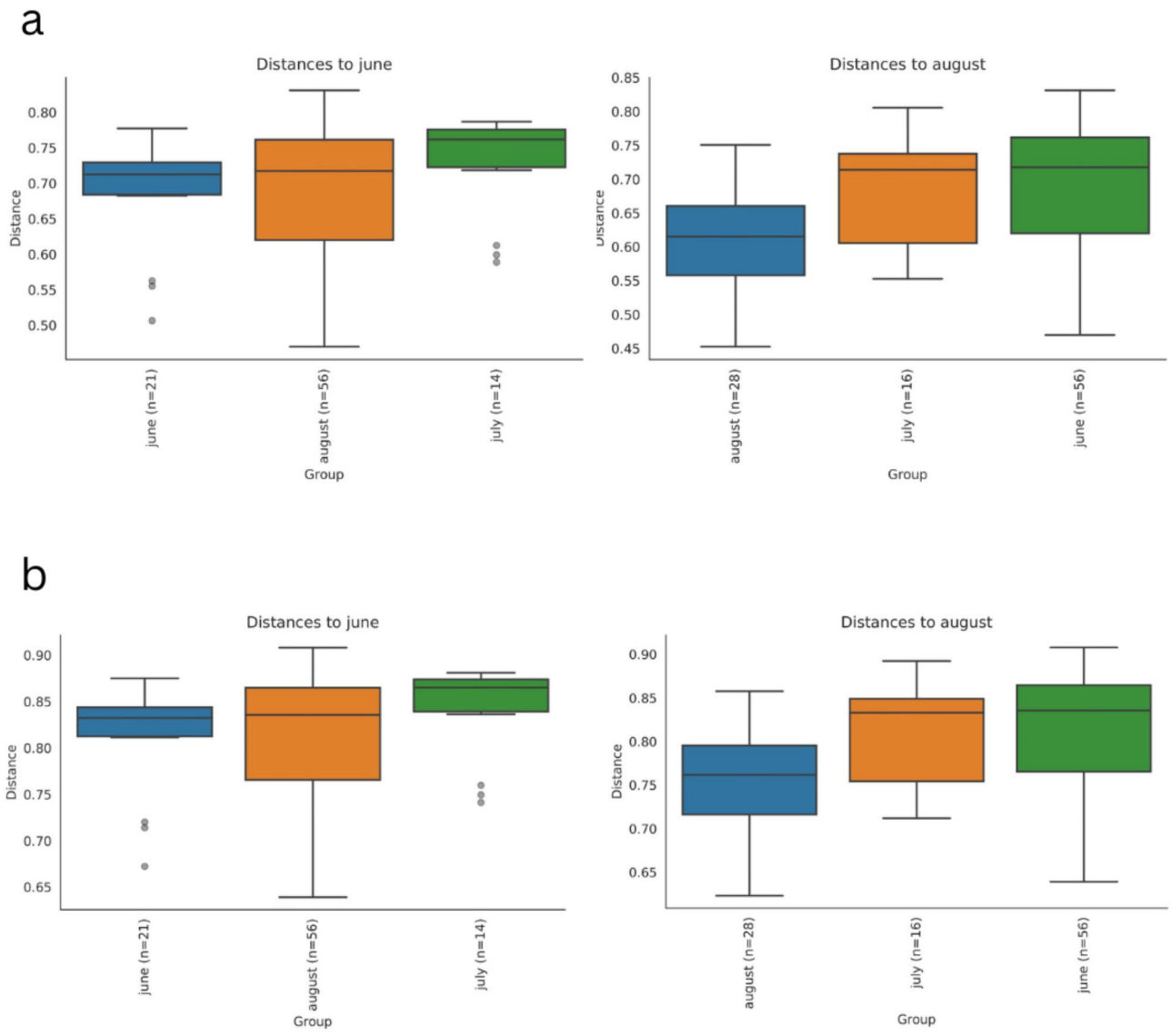

Fig. 4. Box-plots representing β-diversity indexes of Jaccard ($P = 0{,}018$) (**a**) and Dice ($P = 0{,}016$) (**b**) analysis tests (n = number of pairwise comparisons included in the distribution of each group).

observed over time. However, it should be noted that the effects of different biotic and abiotic factors may also be a contributing factor in the formation of these mycobiome profiles.

The samplings in this study were performed in a commercial orchard that was placed in between different fruit cultivating fields. Information has been gained on the application of multisite activity and DMI fungicides along with fertilizers during fruit development (personal communication with orchard's owner). In the region where the sampled orchard is located, it is known that fungicides with different mode of action has been utilized[29] A study investigating the resistance of brown rot pathogens of peaches in Türkiye to some respiratory inhibitor fungicides included samples from Çanakkale/Umurbey[29]. Fungicides are expected to have significant effects on mycobiome composition in terms of both diversity of species and genotype diversity within the species. For example, it has been reported that fungicide applications significantly reduce mycobiome diversity in blueberry fruit skin and pulp[13]. This research plan did not include the direct exploration of the fungicide effect but further studies in this direction are important and necessary. Furthermore, the orchard's owner stated that while fungal diseases, especially brown rot caused by *Monilinia* species and gray mold caused by *Botrytis* species, were a problem in previous years, they have been seen very rarely in recent years. This observation coincided with the observation of a small number of diseased fruits. Fungal diseases, affected by various factors like the protective measures applied or climatic conditions unfavorable for fungal pathogens, point to substantial alterations and dynamics on the fruit surface pathobiome and, of course, the mycobiome.

It was expected that as the fruit matured, some species, especially pathogenic species with host preference or specialization, would become increasingly dominant on the surface as a result of possible competition, establishment and/or infections, thus bringing certain species to the fore and reducing species diversity in the mycobiome. These expectations were supported by taxonomy and diversity analyses that the August samples

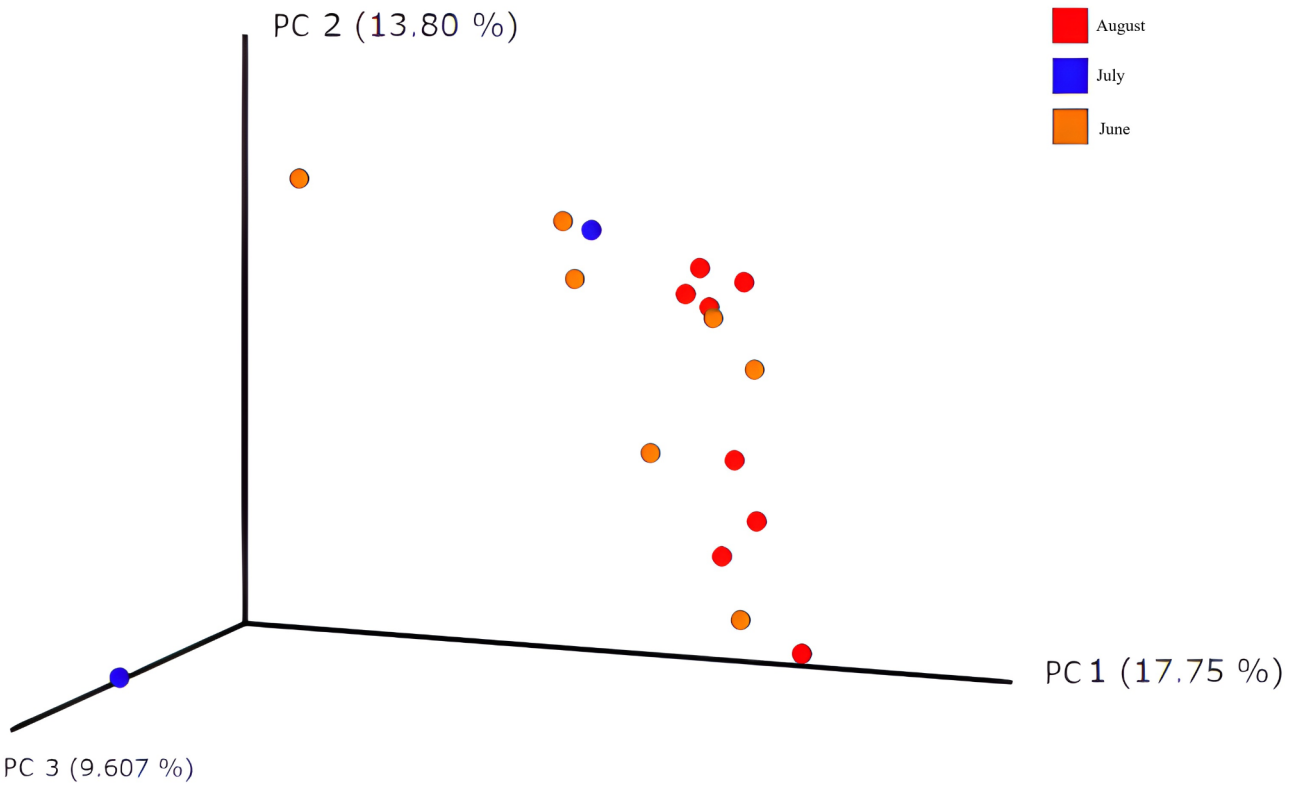

Fig. 5. Bray–Curtis dissimilarity analysis PCoA plot of samples taken each month.

had significantly less diversity than the June samples. Additionally, while the diversity was lowest in August samples, the prevalence of the remaining species was higher. Mainly, *Botrytis cinerea* had a higher abundance rate than other species in June, with *Monilinia fructicola* following close behind. However, in August *Monilinia* species came forward and had the largest abundance rate. It is also important to note that along with June samples having higher *Botrytis* abundance than other sample groups, the diseased Jn3 sample had the highest *Botrytis* abundance and the lowest *Monilina* abundance. The percentages of these species drastically changed in the diseased sample, with *Botrytis cinerea* dominating over the *Monilinia* species, while in the other samples, they were in close competition. This drastic change in the ratio may be related to interspecific competition and/or host–pathogen relationships, such as one species being suppressed by another species and one pathogenic species being more aggressive or faster at infecting the host than the other. These findings support our hypothesis that was formed by the observations in our team's previous research on *Monilinia* species, where brown rot and gray mold diseases were never observed together in fields[18]. The absence of one of the diseases when the other is present is explained in this case study by being both due to seasonal change and the intense competition among the species. It is suggested that as the conditions start to support *Botrytis* at the start of the growing season, the species dominates over *Monilinia fructicola* and diminishes its presence on the surface on a large part. Then as the seasons become more adaptable to *Monilinia fructicola* which has a higher optimal growth temperature than the other, these species start to suppress the other. However, this situation may change based on the population structure of the species in the microenvironment. Genotype effects such as virulence and fungicide resistance levels should also be considered in these interactions.

As the two stated species were in intense competition with one another, other species in the mycobiome fluctuated as well. For example, the *Sclerotinia sclerotiorum* species presence in the samples went down from 8.521 to 6.823% in August, when the *Monilinia fructicola* prevalence was 42.122125% on average. This finding shows that when the abundances of the species change slightly, it may have consequences for other species to stay on the fruit surface and develop. However, species do not always affect each other in negative ways and in some cases, a species prevalence may be beneficial for another to develop[30]. Such was the case for *Sclerotinia tetraspora*, which was only present on the diseased Jn3 sample where the *Botrytis cinerea* prevalence was 63.106%. Although the diseased fruit presents a study case, the presence of this species has the potential to be explained by the stated reason. Another interesting finding was the presence of the *Monilinia polystroma* species. *Monilinia polystroma*, known as the Asiatic brown rot, was reported in Poland[31], China[32], and the Czech Republic[33]. Recently, cases of *Monilinia polystroma* were also reported in Italy as well[34,35]. However, no case of the species has been reported in Türkiye yet, and its presence in peach fruits in Türkiye was detected for the first time in this study, but this was only based on the determination of the presence at the molecular level, and its possible pathogenic effect and infection were not detected. *Monilinia polystroma* was present in all samples from June to August, and the

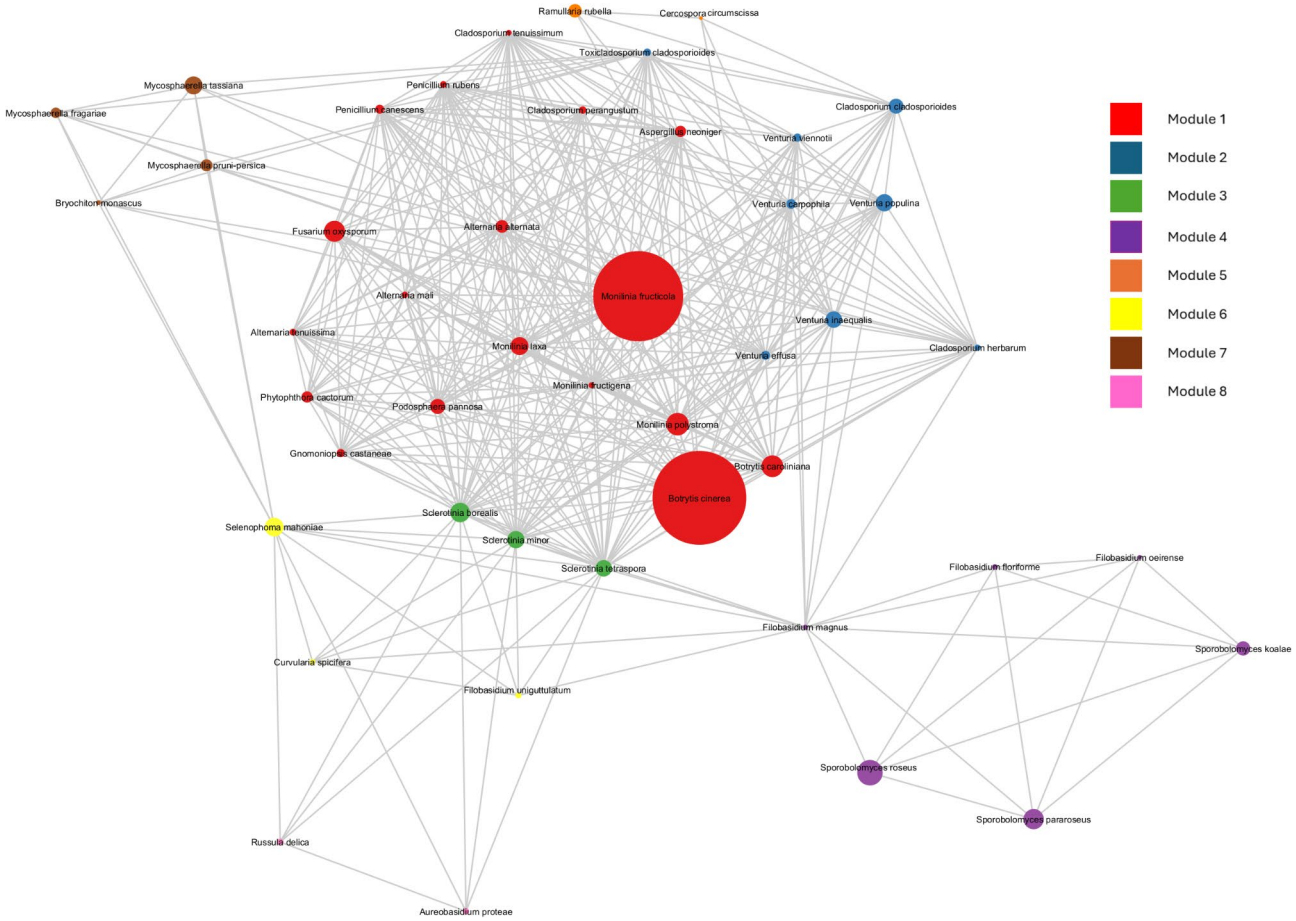

Fig. 6. Co-occurrence network analysis of OTUs throughout the samples. The nodes represent the species, with node sizes correlated to mean abundance percentages. The node colors are in accordance with modules. The lines represent the interaction between nodes.

species was one of the more dominant ones in the mycobiome. This brings attention to the emergence of new diseases as they become more prevalent in their environment and management strategies for disease prevention.

Along with pathogenic species, several non-pathogenic fungal species were also detected. It was observed that the majority of these species were *Basidiomycetes* such as *Sporobolomyces spp.,* which was also directly not present in some of the August samples, suggesting seasonal decrease in its prevalence, and *Filobasidium spp.* while the majority of *Ascomycetes* were pathogenic. In literature, the diversity of fungal species such as the ones stated above are studied extensively, however, most studies are culture-dependent and cultivate the fungal samples before further analyses[9,36]. Although culture-dependent studies are necessary to study fungal organisms extensively, it is important to include unculturable species in biodiversity studies, which cannot be detected with the culture-dependent approaches. By using a culture-independent approach with metabarcoding, we have detected unculturable species such as *Podosphaera spp*., which are obligate biotrophs[37].

Species identified in this study, sampled across different months, exhibited considerable diversity in their ITS region compositions, which was reflected in the ASV diversity of the fungal population within the microenvironment. The ASV diversity within the ITS region did not appear to influence the structuring of species abundance in the mycobiome. Some of the rare species presented themselves in large clusters in the phylogenetic tree with their high ASV diversities, while some of the dominant species presented themselves in smaller clusters in the phylogenetic tree with their low ASV diversities. Moreover, even *B. cinerea*, the most dominant species in the mycobiome, was found to possess a monomorphic ITS region. This observation may imply that the most well-adapted genotypes may be selectively maintained within the populations of dominant species in the mycobiome; however, a deeper understanding requires a large-scale analysis of population structures through metagenomic data.

The network analysis tests have suggested that the fungal species forming the structure identified in this study constantly interact with each other. The main cluster of modules being formed of fungal pathogens also indicates that co-abundance of these pathogens is interconnected. The networks also imply that the presence of one of the species may enable other species of the family to also be present in the mycobiome. These complex interactions among fungal organisms on the fruit surface highlight the need for a more detailed examination, especially in terms of pathogenic species, in understanding the disease formation and development processes, and our further research plan is being prepared in this direction.

In this study, we have shown the dynamicity of the fungal communities on peach fruits at different development stages. Many biotic and abiotic factors at the macro and micro scale, such as physiological changes during the fruit ripening process[38], different biological interactions and molecular traffic of microorganisms both among themselves and with the host[39,40], plant protection practices and different climate effects[41,42], may affect the formation and change of the mycobiome composition. Moreover, the dominance of pathogenic species over the non-pathogenic ones in current conditions show the need for revised disease management strategies. Although fungicides are used against pathogenic fungi, they affect the entire mycobiome[43,44], and the resulting diversity becomes mainly comprised of resistant individuals of pathogenic species such as *Botrytis cinerea* and *Monilinia fructicola*, which showed the highest abundances in the mycobiome structure uncovered here. Considering the structures of the mycobiome appears to offer considerable potential for enhancing the effectiveness of disease management strategies. Correct management of mycobiome composition also appears to be important in disease management strategies. In this direction, planning comprehensive studies involving multiple collaborations from areas such as academia, farmers, agriculture ministries and private sectors will be beneficial for sustainable agriculture.

Materials and method

Sampling

Peach fruit samples were obtained from the target commercial peach orchard located in Umurbey, Çanakkale with the permission of the owner. The orchard was observed from May 2023 when the trees were at the flowering stage, to the end of August 2023 when the last harvest of the fruits was done by the cultivator. The orchard was divided into nine sections and trees at the center of these sections were marked as target trees (Fig. 7). Samplings were performed in June and August 2023 when the fruits were underdeveloped and fully developed (Fig. 8). Fewer fruit samples were also taken in July, when the fruits were partially developed, for better comparison between the sampling times in bioinformatic analyses. As total, 48 fruits were aimed to be taken per sampling time, with 4 samples being taken from each direction profile of a tree. The samples taken from the same tree were pooled to represent the entire profile of the tree. Additionally, the samples taken from the corresponding sections of the orchard were pooled as well to represent the target region. Target region samples were then pooled as given in Table 1, and the samples were named according to their locations in Fig. 7. Furthermore, to ensure that the situation in July, which represents an intermediate stage in the ripening process of the fruit between the June and August samples, was not overlooked, it was planned to collect samples only twice, but with a relatively larger number of samples taken each time (Table 1). Throughout the sampling times, diseased fruits were only encountered in one case, during June sampling at the tree called 7–12. The diseased fruit samples were taken from two profiles of the tree, with other two profiles giving healthy fruits. These fruits were pooled to represent the entirety of the tree like the other samples and included in the profiling. Samples were directly taken to the laboratory for DNA isolation in sterile bags.

DNA isolation, PCR amplification and sequencing

DNA isolation

The isolation procedure started the moment the samples arrived in the laboratory. Circular tissue samples in 1 cm diameter and 2 mm depth were cut from four sites of the sample fruit surfaces with a sterile scalpel. The surface tissues of samples were put together in a sterilized mortar cooled with liquid nitrogen. The fruit tissue samples were crushed with a sterilized pestle and the samples were taken into 2 mL tubes. DNA isolation was performed by using the Norgen Fungi/Yeast Genomic DNA Isolation kit (Norgen, Canada) according to the manufacturer's protocol with minor deviations. Although the entire protocol was followed, each of the centrifuge procedures during the isolation were performed at 14,000 rpm for 2 min to precipitate smaller particles in the initial stages, and then to allow flowthrough to pass from the filter tubes completely. DNA samples were kept in store at -20 °C for further procedures.

Full ITS region amplification and sequencing

The commonly used full ITS region was used for the amplification procedure of the total DNA obtained from the samples to be able to target all organisms within the sample without losing diversity. To test the specificity of the primers to the fungal organisms, previous to the PCR amplifications, *Prunus persica* whole genome available under the BioProject number PRJNA31227[45] was used to map the primers to the genome by using the Geneious 9.1.8[46], where the primers did not align with the genome and no product could be observed in within the target length of 650 bp. Broad spectrum ITS1F/ITS4B primers developed by White et al.[47] and Gardes and Bruns[48] were used to amplify the ITS1-5.8S-ITS2 region specific to fungal species. These primers were also essential in disposing of the DNA of the dead organisms that may be present in the samples, as the target length of the primers surpassed the length of decaying DNA[49].

PCR amplifications of the target region for the samples were carried out as follows; 1 × DreamTaq™ buffer without $MgCl_2$, 0.2 mM dNTPs, 2 mM $MgCl_2$, 0.3 µM of each primer, and 1U DreamTaq™ polymerase was used. 2 µL DNA template was used for each sample and ddH_2O was added to the reaction solution, making the final volume in the PCR tubes 50 µL. Conditions for the PCR amplification were an initial denaturation at 95 °C for 2 min, 40 cycles at 95 °C for 30 s, 54 °C for 45 s, 72 °C for 1 min, and a final extension stage at 72 °C for 5 min.

The amplifications were tested with gel electrophoresis and ultraviolet (UV) visualization was performed with 1.5% gel including 5 µL/100 µL RedSafe™. Samples were run in the gel for 45 min at 100 V and 120 mA. The resulting visualizations have shown that products were obtained with success, with bands being seen in the 650 bp region of the ladders, which corresponds to the target size of the primers.

The PCR reactions were performed in replicates for each sample and the amplification products were sent to Macrogen (Amsterdam, The Netherlands) for library preparation and sequencing using a NovaSeq sequencer.

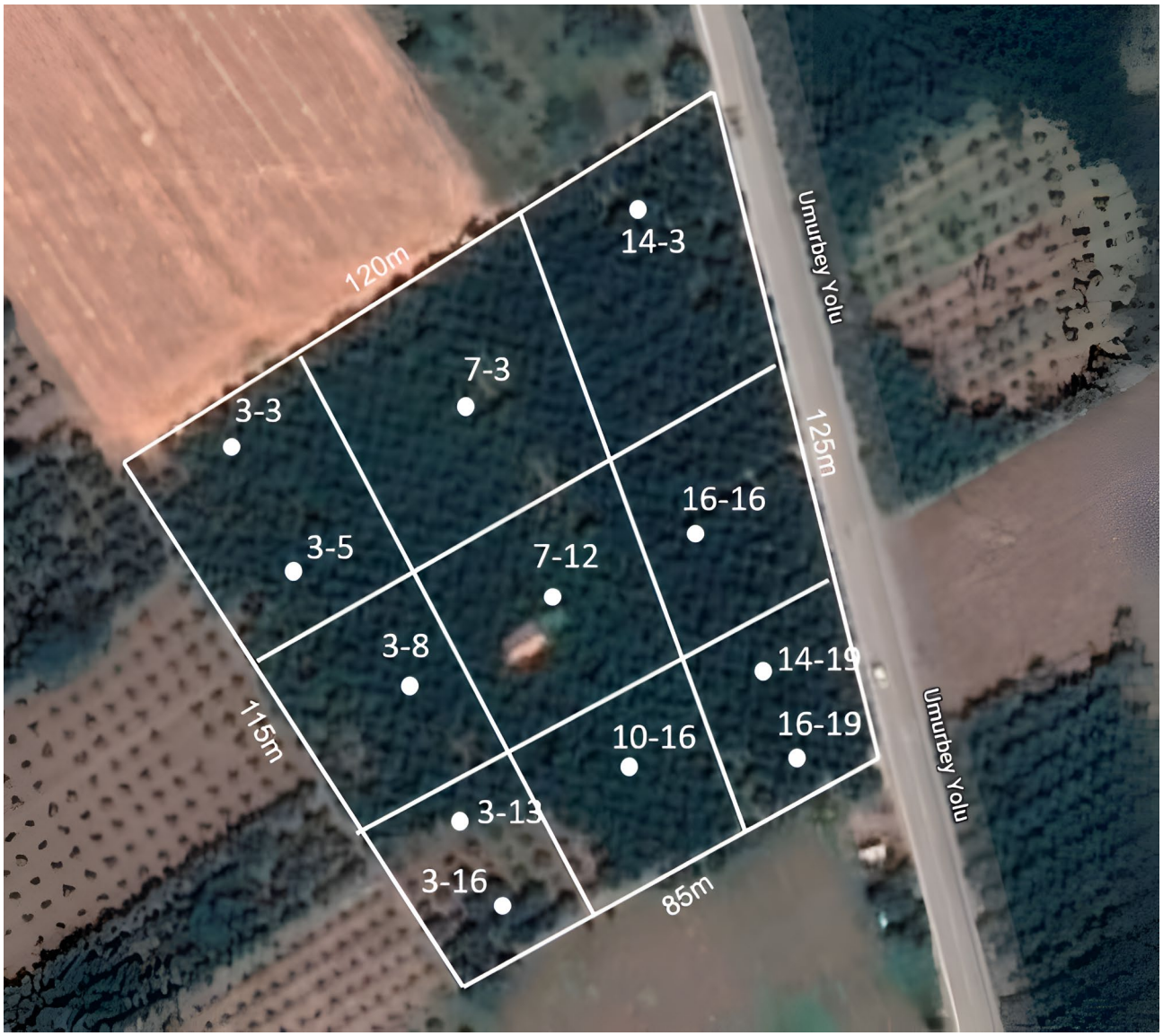

Fig. 7. Target orchard in Umurbey, Çanakkale[70]. Division of the sections for samplings (indicated by lines) and target trees (indicated by dots). Sample locations are given as row and column numbers (Google (n. d.)).

The DNA samples that passed the company's library preparation and sequencing quality filters were sequenced. The samples were multiplexed and normalized during the sequencing to prevent diversity loss.

Statistical and bioinformatic analyses

Raw data analyses

The metabarcoding datasets were analyzed using the QIIME2 2024.2[50] workflow. To summarize, the raw paired-end sequences were demultiplexed with "q2-demux" and the sequencing barcodes were removed from the sequences by using Cutadapt 3.4[51]. Demultiplexed and trimmed sequences were denoised, and corrected, and the chimeras were removed on paired end using DADA2[23] through the "q2-dada2" function.

Taxonomic assignment

A new classifier was trained to make taxonomic assignments for amplicon sequence variants (ASVs). All ITS data was pulled from UNITE 9.0[52] through RESCRIPt[53] including all eukaryotes. The Naive-Bayes classifier was filtered and trained using the "q2-fit-classifier-naive-bayes" function with the classifier being evaluated using the "q2-evaluate-taxonomy" function before taxonomic assignment. The evaluation step enabled the classifier's accuracy to be tested internally, where the testing stages were performed on UNITE 9.0 ITS sequence database, ensuring that the final iteration of the classifier was able to correctly identify all sequences in the given database before its usage in the taxonomic assignment. The taxonomic assignment was done with the newly trained classifier. The classifier was then employed to assign taxonomic annotations to the sample sequences with QIIME2 "classify-sklearn" function. After the annotations were performed, the unidentified taxa, along with

Fig. 8. Development stages of peach fruit samples on sampling groups ((**a**) underdeveloped in June, (**b**) partially developed in July, and (**c**) fully developed in August)).

Sample Name	Pooled samples (coordinates)
A1	3–3, 7–3
A2	14–3, 16–16
A3	7–12
A4	14–19, 16–19
A5	10–16
A6	3–16
A7	3–13, 3–8
A8	3–8, 3–5
Jl1	3–8, 3–5, 3–3, 7–3, 14–3, 7–12
Jl2	16–16, 14–19, 16–19, 10–16, 3–16, 3–13
Jn1	3–3, 7–3
Jn2	14–3, 16–16
Jn3*	7–12*
Jn4	14–19, 16–19
Jn5	10–16
Jn6	3–13, 3–16
Jn7	3–8, 3–5

Table 1. Pooling system of samples from each month. Samples have been coded according to their coordinates given in Fig. 6. (Jn = June, Jl = July, A = August) (The sample including diseased fruits have been indicated with asterisks (*)).

human contaminant taxa were removed from the plot with "qiime taxa filter-table" function. The remaining taxa were considered to form the mycobiome and the relative abundance calculations were based on this normalization. The taxonomic assignment bar plots were obtained through the "q2-taxa-barplot" function after the annotations were filtered.

Alpha and beta diversity analyses

Alpha-diversity metrics Shannon[54] and Berger-Parker[55] dominance indexes were estimated using the "q2-diversity" function. For better visualization, the resulting boxplots were edited using R[56] and R package

"ggplot2"[57] on Rstudio[58]. For beta-diversity analyses, Dice[59] and Jaccard[60] distances were calculated through pairwise PERMANOVA with 999 permutations. The diversity indexes were calculated after a rarefaction curve was plotted using "q2-alpha-rarefaction" to verify the sufficiency of the sequences in presenting the fungal diversity within the samples. The observed feature count per sequence data was plotted using the aforementioned function as well.

EMPeror[61] plugin within QIIME2 was used to visualize the beta diversity patterns among samples based on Bray–Curtis dissimilarities as Principal Coordinates analysis plot (PCoA).

Phylogenetic analyses

All ASVs were aligned using mafft[62] through q2-alignment and the phylogenetic tree of all assigned taxa was obtained using RaxML[63] after the alignment was exported and the evolution model calculated using MrModelTest2[64]. The assigned evolution model of the data set was GTR-Γ, and the maximum likelihood (ML) based phylogenetic tree of the ASVs was built according to the model with 1000 rapid bootstrap and random seeds by using the "q2-phylogeny-raxml" function. The phylogenetic tree was then midpoint rooted and exported using the export function in QIIME2. The bootstrap threshold was then set to 70% and the consensus tree was visualized. The visualized tree contained too many clusters and formed a complex structure, so to raise the interpretability of the tree, the ASVs belonging to the same species were clustered. The visualization and toggling of the tree were performed by using phyloXML[65].

Co-abundance network analysis

Fungal co-abundance network analysis was performed based on the OTU tables and relative abundances of the species in the samples. The pairwise correlations between ASV taxa were calculated with SparCC[66] and the network was built by using SCNIC (version 2020.10)[67,68] with minimum R value of 0.35. Visualization of the network was performed through Cystoscape 3.10.3[69].

Data availability

The data generated and used in this study are available in NCBI GenBank under the BioProject accession number PRJNA1145258.

Received: 5 October 2024; Accepted: 4 March 2025
Published online: 15 March 2025

References

1. Cui, L., Morris, A. & Ghedin, E. The human mycobiome in health and disease. *Genome Med.* **5**(7), 63. https://doi.org/10.1186/gm467 (2013).
2. Kariman, K., Barker, S. J. & Tibbett, M. Structural plasticity in root-fungal symbioses: Diverse interactions lead to improved plant fitness. *PeerJ* **6**, e6030. https://doi.org/10.7717/peerj.6030 (2018).
3. Zhang, Y. et al. Fungi-nematode interactions: Diversity, ecology, and biocontrol prospects in agriculture. J. Fungi 6(4), 206. https://doi.org/10.3390/jof6040206 (2020).
4. Dighton, J. *Fungi in Ecosystem Processes* (CRC Press eBooks, 2018). https://doi.org/10.1201/9781315371528.
5. Moënne-Loccoz, Y., Mavingui, P., Combes, C. & Steinberg, C. Microorganisms and Biotic Interactions. 395–444 (Springer eBooks, 2014). https://doi.org/10.1007/978-94-017-9118-2_11
6. Nilsson, R. H. et al. Mycobiome diversity: High-throughput sequencing and identification of fungi. *Nat. Rev. Microbiol.* **17**(2), 95–109. https://doi.org/10.1038/s41579-018-0116-y (2018).
7. Tiew, P. Y. et al. The mycobiome in health and disease: Emerging concepts, methodologies and challenges. *Mycopathologia* **5**, 156. https://doi.org/10.1007/s11046-019-00413-z (2020).
8. Porras-Alfaro, A. & Bayman, P. Hidden fungi, emergent properties: Endophytes and microbiomes. *Annu. Rev. Phytopathol.* **49**(1), 291–315. https://doi.org/10.1146/annurev-phyto-080508-081831 (2011).
9. Vignassa, M. et al. Pineapple mycobiome related to fruitlet core rot occurrence and the influence of fungal species dispersion patterns. *J. Fungi* **7**(3), 175. https://doi.org/10.3390/jof7030175 (2021).
10. Pozo, M. J., Zabalgogeazcoa, I., De Aldana, B. R. V. & Martinez-Medina, A. Untapping the potential of plant mycobiomes for applications in agriculture. *Curr. Opin. Plant Biol.* **60**, 102034. https://doi.org/10.1016/j.pbi.2021.102034 (2021).
11. Bösch, Y. et al. Dynamics of the apple fruit microbiome after harvest and implications for fruit quality. *Microorganisms* **9**(2), 272. https://doi.org/10.3390/microorganisms9020272 (2021).
12. Setati, M. E., Jacobson, D. & Bauer, F. F. Sequence-based analysis of the *Vitis vinifera* L. cv cabernet sauvignon grape must mycobiome in three South African vineyards employing distinct agronomic systems. *Front. Microbiol.* https://doi.org/10.3389/fmicb.2015.01358 (2015).
13. Szymanski, S. et al. The blueberry fruit mycobiome varies by tissue type and fungicide treatment. *Phytobiomes J.* **7**(2), 208–219. https://doi.org/10.1094/pbiomes-04-22-0028-fi (2023).
14. Piombo, E. et al. Characterizing the fungal microbiome in date (*Phoenix dactylifera*) fruit pulp and peel from early development to harvest. *Microorganisms* **8**(5), 641. https://doi.org/10.3390/microorganisms8050641 (2020).
15. Bill, M., Viljoen, F., Chidamba, L., Gokul, J. & Korsten, L. Fungal microbiome shifts of avocado fruit from flowering to the ready-to-eat stage. *Acta Hortic.* **1363**, 59–68. https://doi.org/10.17660/actahortic.2023.1363.9 (2023).
16. TURKSTAT, Turkish Statistical Institute. Accessed 9 June 2024; https://www.tuik.gov.tr/. (2023).
17. Bayav, A. & Çetinbaş, M. Peach production and foreign trade of Turkey: Current situation, forecasting and analysis of competitiveness. *Anadolu Ege Tarımsal Araştırma Enstitüsü Dergisi* **31**(2), 212–225. https://doi.org/10.18615/anadolu.1033597 (2021).
18. Ozkilinc, H. et al. Species diversity, mating type assays and aggressiveness patterns of Monilinia pathogens causing brown rot of peach fruit in Turkey. *Eur. J. Plant Pathol.* **157**(4), 799–814. https://doi.org/10.1007/s10658-020-02040-7 (2020).
19. Jo, Y., Back, C. G., Choi, H. & Cho, W. K. Comparative microbiome study of mummified peach fruits by metagenomics and metatranscriptomics. *Plants* **9**(8), 1052. https://doi.org/10.3390/plants9081052 (2020).
20. Bien, S. & Damm, U. Prunus trees in Germany—A hideout of unknown fungi?. *Mycol. Progress* **19**(7), 667–690. https://doi.org/10.1007/s11557-020-01586-4 (2020).
21. Ren, N., Dong, N. & Yan, N. Organs, cultivars, soil, and fruit properties affect structure of endophytic mycobiota of pinggu peach trees. *Microorganisms* **7**(9), 322. https://doi.org/10.3390/microorganisms7090322 (2019).

22. Newberger, D. R., Minas, I. S., Manter, D. K. & Vivanco, J. M. A microbiological approach to alleviate soil replant syndrome in peaches. *Microorganisms* **11**(6), 1448. https://doi.org/10.3390/microorganisms11061448 (2023).
23. Callahan, B. J. et al. DADA2: High-resolution sample inference from Illumina amplicon data. *Nat. Methods* **13**(7), 581–583. https://doi.org/10.1038/nmeth.3869 (2016).
24. Hoist-Jensen, A., Vaage, M. & Schumacher, T. An approximation to the phylogeny of Sclerotinia and related genera. *Nord. J. Bot.* **18**(6), 705–719. https://doi.org/10.1111/j.1756-1051.1998.tb01553.x (1998).
25. Gdanetz, K. & Trail, F. The wheat microbiome under four management strategies, and potential for endophytes in disease protection. *Phytobiomes J.* **1**(3), 158–168. https://doi.org/10.1094/pbiomes-05-17-0023-r (2017).
26. Paiva, D. S. et al. Uncovering the fungal diversity colonizing limestone walls of a forgotten monument in the central region of Portugal by high-throughput sequencing and culture-based methods. *Appl. Sci.* **12**(20), 10650. https://doi.org/10.3390/app122010650 (2022).
27. Purahong, W. et al. Characterization of unexplored deadwood mycobiome in highly diverse subtropical forests using culture-independent molecular technique. *Front. Microbiol.* https://doi.org/10.3389/fmicb.2017.00574 (2017).
28. Wijayawardene, N. N. et al. Current insight into culture-dependent and culture-independent methods in discovering ascomycetous taxa. *J. Fungi* **7**(9), 703. https://doi.org/10.3390/jof7090703 (2021).
29. Durak, M. R., Arslan, K., Silan, E., Yildiz, G. & Ozkilinc, H. A novel approach for in vitro fungicide screening and the sensitivity of Monilinia populations from peach orchards in Turkey to respiratory inhibitor fungicides. *Crop Prot.* **147**, 105688. https://doi.org/10.1016/j.cropro.2021.105688 (2021).
30. Mendes, R., Garbeva, P. & Raaijmakers, J. M. The rhizosphere microbiome: Significance of plant beneficial, plant pathogenic, and human pathogenic microorganisms. *FEMS Microbiol. Rev.* **37**(5), 634–663. https://doi.org/10.1111/1574-6976.12028 (2013).
31. Poniatowska, A., Michalecka, M. & Puławska, J. Genetic diversity and pathogenicity of *Monilinia polystroma*—The new pathogen of cherries. *Plant Pathol.* **65**(5), 723–733. https://doi.org/10.1111/ppa.12463 (2015).
32. Zhu, X. Q. & Guo, L. Y. First report of brown rot on plum caused by *Monilinia polystroma* in China. *Plant Disease* **94**(4), 478. https://doi.org/10.1094/pdis-94-4-0478a (2010).
33. Vasić, M., Duduk, N. & Ivanović, M. S. First report of brown rot caused by *Monilia polystroma* on apple in Serbia. *Plant Disease* **97**(1), 145. https://doi.org/10.1094/pdis-07-12-0670-pdn (2013).
34. Deltedesco, E., Oettl, S. & Spitaler, U. First report of brown rot caused by *Monilinia polystroma* on sweet cherry and almond in Italy. *Plant Disease* **107**(7), 2252. https://doi.org/10.1094/pdis-10-22-2482-pdn (2023).
35. Spitaler, U., Oettl, S. & Deltedesco, E. First report of brown rot caused by *Monilinia polystroma* on quince in Italy. *Plant Disease* **107**(1), 229. https://doi.org/10.1094/pdis-06-22-1442-pdn (2023).
36. Gautam, A. K. et al. Current insight into traditional and modern methods in fungal diversity estimates. *J. Fungi* **8**(3), 226. https://doi.org/10.3390/jof8030226 (2022).
37. Polonio, L., Seoane, P., Claros, M. G. & Pérez-García, A. The haustorial transcriptome of the cucurbit pathogen *Podosphaera xanthii* reveals new insights into the biotrophy and pathogenesis of powdery mildew fungi. *BMC Genom.* https://doi.org/10.1186/s12864-019-5938-0 (2019).
38. Prusky, D. & Romanazzi, G. Induced resistance in fruit and vegetables: A host physiological response limiting postharvest disease development. *Annu. Rev. Phytopathol.* **61**(1), 279–300. https://doi.org/10.1146/annurev-phyto-021722-035135 (2023).
39. Bahram, M. & Netherway, T. Fungi as mediators linking organisms and ecosystems. *FEMS Microbiol. Rev.* https://doi.org/10.1093/femsre/fuab058 (2021).
40. Liu, X. & Zhang, Z. A double-edged sword: reactive oxygen species (ROS) during the rice blast fungus and host interaction. *FEBS J.* **289**(18), 5505–5515. https://doi.org/10.1111/febs.16171 (2021).
41. Hanson, M., Petch, G., Ottosen, T. & Skjøth, C. Climate change impact on fungi in the atmospheric microbiome. *Sci. Total Environ.* **830**, 154491. https://doi.org/10.1016/j.scitotenv.2022.154491 (2022).
42. Liu, Z. et al. Elevated CO2 and temperature increase arbuscular mycorrhizal fungal diversity, but decrease root colonization, in maize and wheat. *Sci. Total Environ.* **873**, 162321. https://doi.org/10.1016/j.scitotenv.2023.162321 (2023).
43. Han, L. et al. Deciphering the diversity, composition, function, and network complexity of the soil microbial community after repeated exposure to a fungicide boscalid. *Environ. Pollut.* **312**, 120060. https://doi.org/10.1016/j.envpol.2022.120060 (2022).
44. Sumbula, V., Kurian, P. S., Girija, D. & Cherian, K. A. Impact of foliar application of fungicides on tomato leaf fungal community structure revealed by metagenomic analysis. *Folia Microbiologica* **67**(1), 103–108. https://doi.org/10.1007/s12223-021-00920-x (2021).
45. Verde, I. et al. The high-quality draft genome of peach (*Prunus persica*) identifies unique patterns of genetic diversity, domestication and genome evolution. *Nat. Genet.* **45**(5), 487–494. https://doi.org/10.1038/ng.2586 (2013).
46. Geneious 9.1.8. https://www.geneious.com
47. White, T., Bruns, T., Lee, S., & Taylor, J. Amplıficatıon and dırect sequencıng of fungal rıbosomal RNA genes for phylogenetıcs. 315–322 (Elsevier eBooks, 1990b). https://doi.org/10.1016/b978-0-12-372180-8.50042-1
48. Gardes, M. & Bruns, T. D. ITS primers with enhanced specificity for basidiomycetes—application to the identification of mycorrhizae and rusts. *Mol. Ecol.* **2**(2), 113–118. https://doi.org/10.1111/j.1365-294x.1993.tb00005.x (1993).
49. Jo, T., Takao, K. & Minamoto, T. Linking the state of environmental DNA to its application for biomonitoring and stock assessment: Targeting mitochondrial/nuclear genes, and different DNA fragment lengths and particle sizes. *Environ. DNA* **4**(2), 271–283. https://doi.org/10.1002/edn3.253 (2021).
50. Bolyen, E. et al. Reproducible, interactive, scalable and extensible microbiome data science using QIIME 2. *Nat. Biotechnol.* **37**(8), 852–857. https://doi.org/10.1038/s41587-019-0209-9 (2019).
51. Martin, M. Cutadapt removes adapter sequences from high-throughput sequencing reads. *EMBnet J.* **17**(1), 10. https://doi.org/10.14806/ej.17.1.200 (2011).
52. Abarenkov, K. et al. The UNITE database for molecular identification and taxonomic communication of fungi and other eukaryotes: sequences, taxa, and classifications reconsidered. *Nucleic Acids Res.* **52**(D1), D791–D797. https://doi.org/10.1093/nar/gkad1039 (2023).
53. Robeson, M. S. et al. RESCRIPt: Reproducible sequence taxonomy reference database management. *PLOS Comput. Biol./PLoS Comput. Biol.* **17**(11), e1009581. https://doi.org/10.1371/journal.pcbi.1009581 (2021).
54. Shannon, C. E. A mathematical theory of communication. *Bell Syst. Tech. J.* **27**(3), 379–423. https://doi.org/10.1002/j.1538-7305.1948.tb01338.x (1948).
55. Berger, W. H. & Parker, F. L. Diversity of planktonic foraminifera in deep-sea sediments. *Science* **168**(3937), 1345–1347. https://doi.org/10.1126/science.168.3937.1345 (1970).
56. R Core Team. R: A language and environment for statistical computing (R Foundation for Statistical Computing, 2021). https://www.R-project.org/
57. Wickham, H. *ggplot2: Elegant Graphics for Data Analysis* (Springer-Verlag, 2016). https://ggplot2.tidyverse.org
58. RStudio Team. *RStudio: Integrated Development for R* (RStudio, PBC, 2020). http://www.rstudio.com/
59. Dice, L. R. Measures of the amount of ecologic association between species. *Ecology* **26**(3), 297–302. https://doi.org/10.2307/1932409 (1945).
60. Jaccard, P. Nouvellesrecherches sur la distribution florale. *Bull. Soc. V Sci. Nat.* **44**, 223–270 (1908).
61. Vázquez-Baeza, Y., Pirrung, M., Gonzalez, A. & Knight, R. EMPeror: A tool for visualizing high-throughput microbial community data. *Gigascience* https://doi.org/10.1186/2047-217x-2-16 (2013).

62. Katoh, K. & Standley, D. M. MAFFT multiple sequence alignment software version 7: Improvements in performance and usability. *Mol. Biol. Evolut.* **30**(4), 772–780. https://doi.org/10.1093/molbev/mst010 (2013).
63. Stamatakis, A. RAxML version 8: A tool for phylogenetic analysis and post-analysis of large phylogenies. *Bioinformatics* **30**(9), 1312–1313. https://doi.org/10.1093/bioinformatics/btu033 (2014).
64. Nylander, J. A. A. MrModeltest v2. Program distributed by the author. Evolutionary Biology Centre, Uppsala University (2004).
65. Han, M. V. & Zmasek, C. M. phyloXML: XML for evolutionary biology and comparative genomics. *BMC Bioinform.* https://doi.org/10.1186/1471-2105-10-356 (2009).
66. Friedman, J. & Alm, E. J. inferring correlation networks from genomic survey data. *PLoS Comput. Biol.* **8**(9), e1002687. https://doi.org/10.1371/journal.pcbi.1002687 (2012).
67. Shaffer, M., Thurimella, K., Sterrett, J. D. & Lozupone, C. A. SCNIC: Sparse correlation network investigation for compositional data. *Mol. Ecol. Resour.* **23**(1), 312–325. https://doi.org/10.1111/1755-0998.13704 (2022).
68. Shaffer, M., Thurimella, K., Sterrett, J. D. & Lozupone, C. A. SCNIC: Sparse correlation network investigation for compositional data. *Mol. Ecol. Resour.* https://doi.org/10.1111/1755-0998.13704 (2020).
69. Shannon, P. et al. Cytoscape: A software environment for integrated models of biomolecular interaction networks. *Genome Res.* **13**(11), 2498–2504. https://doi.org/10.1101/gr.1239303 (2003).
70. Google Maps [View of the target orchard in Umurbey/Çanakkale], accessed 27 July 2024; https://goo.gl/maps

Acknowledgements
The authors thank to Scientific Research Project Coordination Unit of Çanakkale Onsekiz Mart University (Project No: FYL-2023-4385) for their financial supports. The authors would like to thank all Özkılınç lab members for their helps whenever needed throughout the project.

Author contributions
SO performed the sampling, laboratory work, and bioinformatics analysis and writing of the article in consultation with HO. HO directed the research, recommended, and reviewed data analyses, contributed to all phases of the research and manuscript writing. Both authors read, discussed, and approved the manuscript.

Funding
This work was supported by the Scientific Research Project Coordination Unit of Çanakkale Onsekiz Mart University (Project No: FYL-2023-4385).

Declarations

Competing interests
The authors declare no competing interests.

Ethics approval and consent to participate
All experiments conducted in this study do not require ethics approval.

Additional information
Supplementary Information The online version contains supplementary material available at https://doi.org/10.1038/s41598-025-93090-6.

Correspondence and requests for materials should be addressed to H.Ö.

Reprints and permissions information is available at www.nature.com/reprints.

Publisher's note Springer Nature remains neutral with regard to jurisdictional claims in published maps and institutional affiliations.